

# Demonstration of Etch-less Core Definition Process for Low-Loss Glass Waveguide Fabrication

Demis D. John, Renan Moreira, Jonathon S. Barton, Jared F. Bauters,  
 Martijn J. R. Heck, John E. Bowers and Daniel J. Blumenthal  
 Electrical & Computer Engineering Department  
 University of California Santa Barbara, Santa Barbara, California, U.S.A.  
 demis@engineering.ucsb.edu

**Abstract**— We demonstrate for the first time the selective oxidation of Silicon Oxynitride and use it to create a novel process for etchless waveguide definition. The oxidation process is characterized for  $\text{SiO}_x\text{N}_y$  and  $\text{Si}_3\text{N}_4$  films, and the sidewall smoothing mechanism is simulated. Fabricated waveguides exhibited losses of 0.103 dB/cm at 1610 nm and 0.177 dB/cm at 1550 nm, where C-band loss were limited by molecular vibrational resonances.

**Keywords:** Waveguides, Thermal Oxidation, Silicon Oxynitride

## I. INTRODUCTION

The large disparity between the propagation losses of optical fibers and planar waveguides is often attributed to the sidewall roughness of integrated waveguides, created by the etching process. In the silicon-on-insulator platform, numerous groups have addressed this problem with the local oxidation of silicon (LOCOS) [1-4] process, which reduces propagation loss by about an order of magnitude.

The Silicon Oxynitride ( $\text{SiO}_x\text{N}_y$ ) / Silicon Dioxide ( $\text{SiO}_2$ ) planar lightwave circuit (PLC) platform is a mature technology for various applications, in which the oxynitride mole ratio can be varied to tailor the core refractive index.  $\text{SiO}_x\text{N}_y$  can also be thermally oxidized [5,6], and it stands to reason that a similar sidewall smoothing technique can be applied to the ubiquitous  $\text{SiO}_x\text{N}_y/\text{SiO}_2$  glass waveguide platform to define waveguides with reduced sidewall roughness.

In this work we present a characterization of the thermal oxidation of  $\text{SiO}_x\text{N}_y$  using spectroscopic ellipsometry, with relation to the chemical processes involved. Additionally, a model for the mechanism of sidewall smoothing is proposed using a 1-dimensional approximation of the diffusion of oxidant species. This is then applied to the fabrication of  $\text{SiO}_x\text{N}_y$  waveguides of varying widths, which are subsequently measured with optical frequency domain reflectometry (OFDR) to obtain wavelength-dependent losses [7]. Lastly, the loss spectrum is used to infer the presence of various molecular absorption resonances.

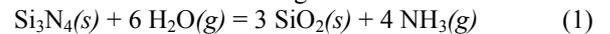
## II. SELECTIVE OXIDATION OF SILICON OXYNITRIDE

In a standard LOCOS process, a material with low oxidation rate is used to block the diffusion of oxidant in lithographically defined areas, allowing exposed silicon to oxidize. In the case of  $\text{SiO}_x\text{N}_y$  waveguides with  $\text{SiO}_2$  cladding, we can use a layer of  $\text{SiO}_x\text{N}_y$  as the core layer, and block oxidant diffusion in the waveguide core area with  $\text{Si}_3\text{N}_4$ , which is essentially  $\text{SiO}_x\text{N}_y$  with zero oxygen content. Thus the exposed  $\text{SiO}_x\text{N}_y$  is converted into cladding oxide.

Fig. 1 shows a schematic of the core definition process, including the use of thermally oxidized silicon substrates for lower claddings. Deposited  $\text{SiO}_2$  is used for upper claddings after removal of the  $\text{Si}_3\text{N}_4$  oxidation mask.

## III. THERMAL OXIDATION OF SILICON OXYNITRIDE

Kuiper et al. proposed in [6] that Silicon Nitride undergoes thermal oxidation with the following reaction:



where the gaseous oxidant, water vapor, replaces nitrogen within a solid silicon nitride molecule, creating solid silica and gaseous ammonia as a byproduct. The rate of oxidation is limited by out-diffusion of the ammonia molecule, which inhibits the reaction rate at the oxidizing interface. Due to the dependence on diffusion, the rate follows an exponential temperature-dependence. Since each nitrogen atom generates a rate-limiting ammonia molecule, the oxidation rate should be highly dependent on the amount of nitrogen in the  $\text{SiO}_x\text{N}_y$  film. This is exhibited in Fig. 2, where the  $\text{SiO}_x\text{N}_y$  refractive index increases with increasing nitrogen content, and thus shows a lower oxidation rate.

Additionally, water vapor and ammonia will be left in the film at the completion of the thermal oxidation. This fact manifests in two effects impacting waveguide characteristics. First, since  $\text{NH}_3$  is larger and has a lower diffusion coefficient than  $\text{H}_2\text{O}$ , the generated thermal oxide tends to have higher indices (and  $\text{N}_2$  concentration) at low temperatures. This is likely due to the trapping of  $\text{NH}_3$  which allows the thermal oxide to undergo thermal nitridation [8]. Secondly, both of these molecules exhibit molecular vibrational resonances in the C-band, via O-H and N-H overtones, so wavelength dependent loss analysis should be able to detect the residual solute gases.

The effect this technique has on sidewall roughness has been investigated by modeling the diffusion of oxidant as spherical point sources along the line-edge of the etched oxidation mask.

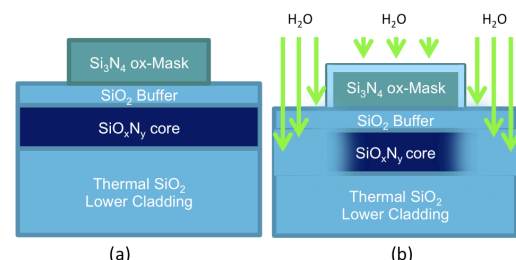


Figure 1. (a) Schematic of waveguide definition via local oxidation of  $\text{SiO}_x\text{N}_y$  showing deposited films & etched oxidation mask. (b) Shows conversion of  $\text{SiO}_x\text{N}_y$  to cladding oxide via thermal steam oxidation.

This research was supported by the Defense Advanced Research Projects Agency, Microsystems Technology Office, Program: Integrated Photonic Delay (iPhoD), Issued by DARPA/CMO under Contract No. HR0011-09-C-0123. The views and conclusions contained in this document are those of the authors only.

In Fig. 3a, we propagate the diffusion front away from the line-edge (as measured with atomic force microscopy), and calculate the resultant root-mean-square (RMS) roughness and correlation length ( $L_c$ ), shown in Fig. 3b. As diffusion radius increases, RMS roughness decreases and  $L_c$  increases. Both of these trends reduce scattering losses [9].

#### IV. WAVEGUIDE FABRICATION & MEASUREMENT

A 1 mm thick silicon substrate with 15  $\mu\text{m}$  of thermal oxide was used for the lower cladding. Plasma Enhanced Chemical Vapor Deposition (PECVD) was used to deposit 970 nm of  $\text{SiO}_x\text{N}_y$  waveguide core layer, with the  $\text{O}_2/\text{N}_2$  gas flow ratio chosen to produce a refractive index of 1.58 at 1550 nm. 1  $\mu\text{m}$  of  $\text{SiO}_2$  was subsequently deposited as an oxidation buffer, and 50 nm of sputtered  $\text{Si}_3\text{N}_4$  for the oxidation mask. Sputtered nitride exhibits a lower oxidation rate than PECVD films, and thus requires less physical etching to pattern. Standard lithographic and dry-etching techniques were used to pattern the oxidation mask with an Archimedean spiral configuration of 26 interleaved waveguides, ranging from 2.5  $\mu\text{m}$  to 15.0  $\mu\text{m}$  in width. Core definition proceeded by subjecting the wafer to steam oxidation for 3 hours at 950°C with a 200 sccm flow of water vapor. The nitride oxidation mask was then removed via dry etch, and 10  $\mu\text{m}$  of PECVD  $\text{SiO}_2$  upper cladding was deposited in batches, with 1050°C, 3hr anneals performed after every 4  $\mu\text{m}$  of deposition. The spiral facets were diced (shown in Fig. 4), and light was coupled from cleaved optical fibers to the waveguides with index matching gel to lower reflections.

OFDR was used to measure the backscattered power versus distance into each waveguide, as described in [7]. Analysis of the power vs. distance slopes of full-range OFDR scans (1525 nm – 1610 nm) yielded the losses shown in Fig. 5a, with a lowest loss of 14.7 dB/m for the widest, 15  $\mu\text{m}$  waveguide. These values are average losses over the OFDR scan range, so narrow-band analysis was performed with a 10 nm range, as shown in Fig. 5b, revealing a 20 dB/m range of propagation losses for the 13.0  $\mu\text{m}$  width. This loss spectrum shows a minimum loss of  $11.2 \pm 0.4$  dB/m from 1585 nm to 1610 nm, and the 15  $\mu\text{m}$  width exhibits  $10.3 \pm 0.8$  dB/m from 1590 nm to 1610 nm. The loss peak near 1510 nm is explained by the presence of N-H vibrational overtones. Losses around 1610 nm could be limited by either scatter or SiO-H & Si-H bonds. This will be determined in the future by fitting the loss vs. width data to scattering loss models.

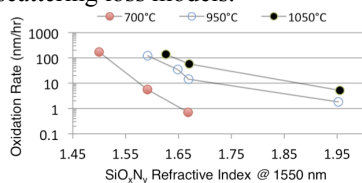


Figure 2. Oxidation rates for a range of temperatures and refractive indices.

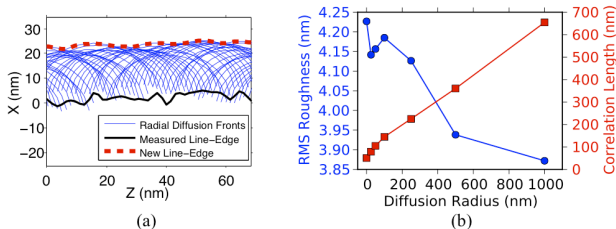


Figure 3. The 1-D simulation is shown in (a), and (b) shows the resulting sidewall roughness RMS (circles) and  $L_c$  (squares) for varying diffusion radii.

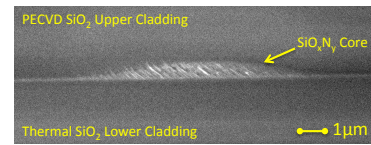


Figure 4. A cross-section image of a 9.5  $\mu\text{m}$  x 0.96  $\mu\text{m}$  waveguide core.

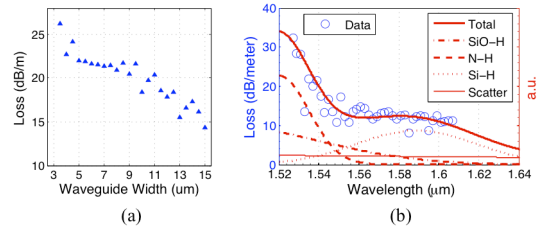


Figure 5. (a) Shows losses averaged over the full OFDR spectral range for each waveguide width, while (b) shows a narrow-wavelength OFDR loss spectrum for the 13.0  $\mu\text{m}$  width, with approximate bond resonances.

#### V. CONCLUSION

We have developed and demonstrated a process for the local oxidation of  $\text{SiO}_x\text{N}_y$ , applied to silica-based waveguides. We modeled the sidewall smoothing mechanism and characterized the oxidation process with regards to the residual nitrogen, temperature and index dependence. Lastly we fabricated and measured the wavelength-dependent losses of  $\text{SiO}_x\text{N}_y$  waveguides showing a minimum loss of  $10.3 \pm 0.4$  dB/m, and revealed the bond resonances dominating losses.

#### ACKNOWLEDGMENT

The authors would like to thank Scott Rodgers, Brandon Knott and Jonathan Doyle for support and helpful discussions.

#### REFERENCES

- [1] L. Rowe, M. Elsey, N. Tarr, A. P. Knights, and E. Post, "CMOS-compatible optical rib waveguides defined by local oxidation of silicon," *Electronics Letters*, vol. 43, no. 7, pp. 392–393, Mar. 2007.
- [2] R. Pafchek, R. Tummid, J. Li, M. A. Webster, E. Chen, and T. L. Koch, "Low-loss silicon-on-insulator shallow-ridge TE and TM waveguides formed using thermal oxidation," *Applied Optics*, vol. 48, no. 5, pp. 958–963, 2009.
- [3] J. Cardenas, C. B. Poitras, J. T. Robinson, K. Preston, L. Chen, and M. Lipson, "Low loss etchless silicon photonic waveguides," *Optics Express*, vol. 17, no. 6, pp. 4752–4757, Mar. 2009.
- [4] M. P. Nezhad, O. Bondarenko, M. Khajavikhan, A. Simic, and Y. Fainman, "Etch-free low loss silicon waveguides using hydrogen silsesquioxane oxidation masks," *Optics Express*, vol. 19, no. 20, pp. 18827–18827, 2011.
- [5] D. Choi, D. B. Fischbach, and W. D. Scott, "Oxidation of Chemically-Vapor-Deposited Silicon Nitride and Single-Crystal Silicon," *Journal of the American Ceramics Society*, vol. 72, no. 7, pp. 1118–1123, 1989.
- [6] A. Kuiper, M. F. C. Willemsen, J. M. L. Mulder, JB Oude Elferink, F. H. P. M. Habraken, and W.F. van der Weg, "Thermal oxidation of silicon nitride and silicon oxynitride films," *J. Vac. Sci. Technol. B*, vol. 7, no. 3, pp. 455–465, May 1989.
- [7] J. F. Bauters, M. J. R. Heck, D. D. John, J. S. Barton, C. M. Bruinink, A. Leinse, R. G. Heideman, D. J. Blumenthal, J. E. Bowers, "Planar waveguides with less than 0.1 dB/m propagation loss fabricated with wafer bonding," *Optics Express*, vol. 19, no. 24, pp. 24090, Nov. 2011.
- [8] Y. Hayafuji and K. Kajiwar, "Nitridation of Silicon and Oxidized-Silicon," *Journal of The Electrochemical Society*, vol. 129, no. 9, pp. 2102–2108, Sep. 1982.
- [9] K. K. Lee, D. R. Lim, H.-C. Luan, A. Agarwal, J. Foresi, and L. C. Kimerling, "Effect of size and roughness on light transmission in a Si/SiO<sub>2</sub> waveguide: Experiments and model," *Applied Physics Letters*, vol. 77, no. 11, pp. 1617–1619, Sep. 2000.